PERGAMON

International Journal of Solids and Structures 38 (2001) 2161–2170

INTERNATIONAL JOURNAL OF SOLIDS and STRUCTURES

www.elsevier.com/locate/ijsolstr

Mechanical model of the pattern formation of lotus receptacles

T. Tarnai *

Department of Structural Mechanics, Faculty of Civil Engineering, Technical University of Budapest, Budapest, Műegyetem rkp. 3., H-1521, Hungary

Received 6 August 1999; in revised form 13 December 1999

Abstract

A two-dimensional mechanical model for pattern formation is described. The lotus receptacle is modelled as a finite circle packing with an elastic boundary of minimum length. The deformation process is controlled by an increase in internal pressure. Equilibrium configurations are sought. During the process, the configuration is sometimes unchanged, sometimes changes continuously, but in some cases, by loss of stability, a dramatic rearrangement of the circles occurs. At the pressure under which the contact forces between circles vanish, the circles form a locally densest packing in a circle.

Keywords: Biomechanics; Circle packing; Pattern formation; Equilibrium configuration; Stability of circle packing

1. Introduction

Sacred lotus (*Nelumbo nucifera*) flowers have a conical receptacle with a circular, even upper surface (Lian, 1987). In that circular face, there are several small depressions, each of which contains one carpel. At first sight, it seems that the carpels are arranged spirally (Watanabe, 1990). On close inspection, however, it was found (Tarnai, 1997) that the arrangement of carpels, and later the arrangement of fruits, in the receptacle is in accordance with the solution to the following mathematical packing problem (Croft et al., 1991; Graham et al., 1998): How must n non-overlapping equal circles be packed in the unit circle so that the diameter of the circles will be as large as possible? Comparing actual fruit arrangements (such as Fig. 1(a)) with the mathematical solutions (such as Fig. 1(b)), the agreement is striking. However, as in living objects, there are always imperfections and mutations, this optimality property of *Nelumbo* receptacles is not a rigid law but only a prevalent tendency. Indeed, we have also found receptacles with fruit arrangements different from the mathematical solution. The basic question here is: How to explain the pattern formation of lotus receptacles?

In developmental biology of plants, there are different theories for answering such questions. According to Thornley (1975), there are two main approaches to the problems of phyllotaxis and primordial initiation.

* Tel.: +36-1-463-1431; fax: +36-1-463-1099.
E-mail address: tarnai@ep-mech.me.bme.hu (T. Tarnai).

0020-7683/01/$ - see front matter
PII: S0020-7683(00)00159-1

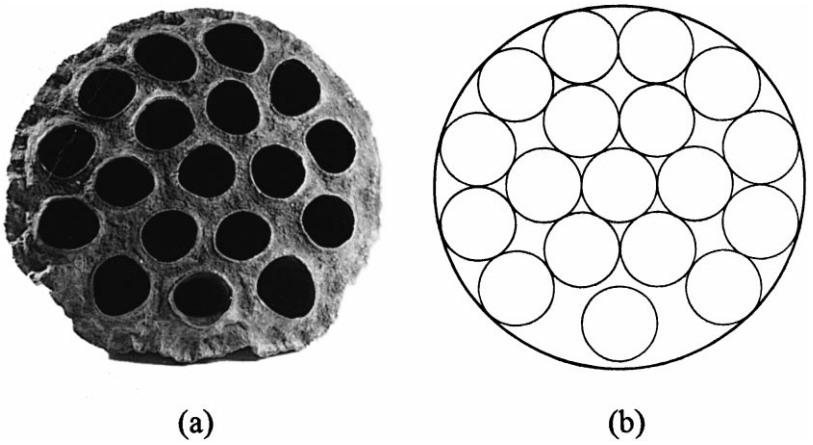

Fig. 1. (a) Arrangement of 18 fruits in the lotus receptacle (depressions in a dried specimen). (b) Densest packing of 18 equal circles in a circle.

The first is the field theory, in which a field can be chemical (reaction–diffusion theory) (Turing, 1952) or physical (buckling theory) (Green, 1996; Green et al., 1996). The second is the packing theory with mechanical-like constraints. The first approach can be effective for the early stage of primordial initiation, but the second approach is better for the later stages of primordial development. Sequential generation of primordia in general results in a spiral phyllotaxis, but simultaneous generation can lead to non-spiral phyllotaxis. These forms come out also from rigorous mathematical analysis (Jean, 1994; Prusinkiewicz and Lindenmayer, 1990).

In the case of lotus receptacles, it is supposed that primordia are generated simultaneously. Then, the mathematical packing model is able to explain the formation of regular patterns (i.e., where the carpels are considered as equal circles, and the upper surface of the receptacle as a circle), but it is not able to describe polymorphism of pattern for any value of $n > 3$ even when the carpels are considered equal. A better model can be obtained if some of the physical–mechanical characteristics of the receptacles are taken into account.

In this paper, we suggest a mechanical model for the pattern formation of the lotus receptacle in the primordial development stage, where packing constraints and the boundary conditions are crucial. The pattern resulting from this model is an equilibrium configuration of equal circles.

2. The mechanical packing model

2.1. Assumptions

The configuration is considered in the plane, where the primordia (carpels) are represented by n equal circles (rigid discs) of radius r, the boundary of the receptacle by a linearly elastic band of strained length L, and turgor by hydrostatic pressure p directed outward. The band has tensile stiffness but no bending stiffness, and the cross-section of the band is constant. The thickness of the band is negligible, compared to the radius of circles. All contacts are frictionless. It is supposed that at the beginning there is no internal pressure, and in the initial configuration, the circles form the densest finite packing (Wills, 1998) in their *convex hull* under the restriction that the length of the boundary of the convex hull is a minimum. (*Density* of finite packing is defined as the ratio of the total area of circles to the area of the convex hull.) If the length of the elastic band in the rest position, L_0, is less than the perimeter of the convex hull, then the band is

tightened, and the system is in a state of self-stress with minimum strain energy. So, we have a packing of n equal circles, whose convex hull has a minimum perimeter, and among the packings with minimum-perimeter convex hulls, we consider the one for which the area of the convex hull is minimum. For small values of n, these circle configurations are similar to those in the book of Hooke (1665) explaining crystal structures.

Suppose that the voids are filled in completely with incompressible fluid that can move freely between the discs, and between discs and the elastic band, even where a disc is in contact with the band. Then, hydrostatic pressure p is introduced under which the elastic band extends and its straight-line segments become circular arcs of radius R, while the tensile force S everywhere in the band is constant (Irvine, 1981). It is supposed that the loading process and the response of the system is quasi-static, i.e., the dynamical effects are neglected. Angles are measured in radians. Under these assumptions, we determine the equilibrium configuration for a given p.

2.2. Equilibrium configuration

Consider a packing of equal circles under hydrostatic pressure in a curved envelope. Although the configuration is controlled physically by pressure p, in the calculation, it is more convenient to take the variable, radius R, of a free segment of the band. Let us suppose that coordinates of centres of the circles are given in a Cartesian coordinate system x, y, and that we know radius R.

We first determine the other geometrical data of the configuration using the notation in Fig. 2(b). Centres of the circles touching the band determine a convex polygon. Let it be denoted by P. If x_i, y_i and x_j, y_j denote the coordinates of centres i and j, then the length of the side of polygon P between vertices i and j is

$$h_{ij} = \sqrt{(x_i - x_j)^2 + (y_i - y_j)^2}. \tag{1}$$

The coordinates of three consecutive vertices j, i, k, in terms of distances (1), determine the angle δ_i of polygon P at vertex i:

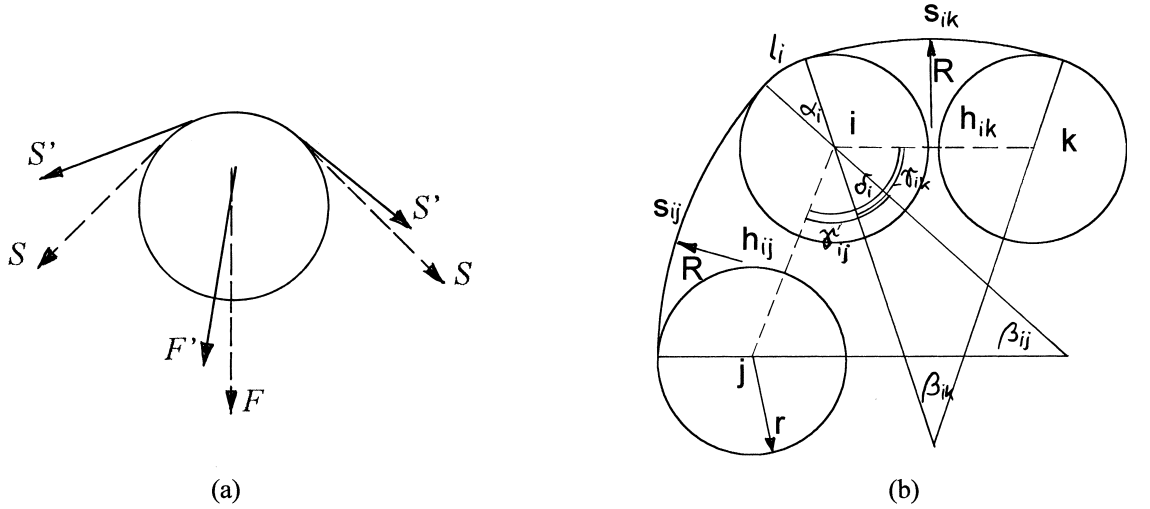

Fig. 2. (a) Change of magnitude and direction of the force in the band. (b) Notation used in calculations.

$$\delta_i = \arccos \frac{h_{ij}^2 + h_{ik}^2 - h_{jk}^2}{2h_{ij}h_{ik}}. \tag{2}$$

Points at which the circle of radius R is tangent to circles i and j define angle β_{ij}:

$$\beta_{ij} = 2\arcsin \frac{h_{ij}}{2(R-r)} \tag{3}$$

and γ_{ij}:

$$\gamma_{ij} = \tfrac{1}{2}(\pi - \beta_{ij}).$$

Determining these angles also from the tangent points on circles i and k, we have

$$\alpha_i = \gamma_{ij} + \gamma_{ik} - \delta_i. \tag{4}$$

From Eqs. (3) and (4), the free segment s_{ij} and the contact segment l_i of the band are obtained:

$$s_{ij} = R\beta_{ij},$$

$$l_i = r\alpha_i.$$

Then, the length of the band in the strained profile, L, is

$$L = \sum_i l_i + \sum_{ij} s_{ij} = r\sum_i \alpha_i + R\sum_{ij} \beta_{ij}, \tag{5}$$

where the summation is extended to all vertices i and all sides ij of polygon P.

We are now in a position to determine forces in the system. Since the unstrained length of the band is L_0, because of Hooke's law, the tensile force S in the band is obtained in the form:

$$S = Ea\left(\frac{L}{L_0} - 1\right), \tag{6}$$

where E is Young's modulus, and a is the uniform cross-sectional area in the unstrained band. The force in the band can be expressed also in terms of the hydrostatic pressure and the radius of a free segment of the band as

$$S = Rp. \tag{7}$$

Eq. (6) is a relationship between force S and radius R. By expressing R from Eq. (7) and introducing it into Eq. (6), we obtain a relationship between force S and hydrostatic pressure p, whence S can be calculated. If, at the boundary, a circle and the band have more than one point in common, then a force F is transmitted to the circle from the band (Fig. 2(a)). At circle i, its value is

$$F_i = 2(S - pr)\sin\frac{\alpha_i}{2}, \tag{8}$$

and its line of action is the bisector of angle α_i. To the packing of non-overlapping equal circles, there corresponds a *graph* (Tarnai and Gáspár, 1995–1996). The vertices of the graph are the centres of the circles, and the edges of the graph are straight-line segments joining the centres of the touching circles. Thus, all edges of the graph are of equal length. In our investigation, the graph is considered as a truss consisting of straight bars and frictionless pin joints. The bars are under unilateral constraints, i.e., they can carry only compressive forces and not tensile forces. (Two circles in contact can be in equilibrium with a compressive contact force, but not with a tensile contact force because under forces, which would cause a tensile contact force, the circles will part from each other.) So, we have a bar-and-joint structure under unilateral constraints, which is loaded at the joints at the boundary as shown in Fig. 6. The task is to

ascertain whether this bar-and-joint structure is in equilibrium. We are looking for equilibrium configurations while pressure p is increased. Under the increase of the internal pressure, the force in the boundary band is increasing from S to S', while the magnitude and the direction of the force F transmitted from the band to a circle at the boundary are changing to those of F' (Fig. 2(a)). The equilibrium of the system under the modified loads should be checked. If the system is not in equilibrium, using an iteration process, the configuration may be modified until the equilibrium is fulfilled.

It can occur that the change of the configuration is better controlled by the area A of the domain bounded by the band than by the radius R. This is the case in particular if there is no internal pressure, i.e., both $p = 0$ and $1/R = 0$. In the case $1/R \neq 0$, the area is

$$A = A_P + \frac{r^2}{2}\sum_i \alpha_i + \frac{1}{2}\sum_{ij}\left(R^2\beta_{ij} - h_{ij}(R-r)\cos\frac{\beta_{ij}}{2}\right), \tag{9}$$

where A_P is the area of polygon P. In the case $1/R = 0$, the area is

$$A = A_P + rL_P + r^2\pi, \tag{10}$$

where L_P is the length of the perimeter of polygon P, $L_P = \sum h_{ij}$.

The equilibrium path of the system under internal pressure can be calculated and plotted as pressure p against area A, or pressure p against radius R. We will show examples of both ways of presenting equilibrium paths.

3. Examples

In the following examples, we suppose that in the minimum-perimeter finite packings of circles, the elastic band is free of stress, i.e., $L_0 = L_P + 2r\pi$. We also suppose that we have unit circles ($r = 1$), and the tensile rigidity of the elastic band is $Ea = 1$. Since we want to analyse the effect of change of pressure in principle, the actual dimensions of different variables have no importance, so the dimensions will not be given in the diagrams (but, for instance, N for Ea, mm for r and R, mm^2 for A, N/mm for p provide a consistent system). Calculations and some of the diagrams were made by using a MATLAB package.

3.1. $n = 3$

In the densest configuration, the three circles are arranged so that the centres are at the vertices of an equilateral triangle, whose side length is equal to the diameter of the circles. This is preserved as the equilibrium configuration while the pressure is increased until the band forms the circumcircle of the packing of the three circles, which is just the mathematical packing model of the pattern for three carpels. By a further increase in the pressure, the configuration becomes indefinite, the circles rattle in the circular band. The same properties characterize the configurations for $n = 7$ and 19. The behaviour of the configuration for $n = 6$ is similar. The only difference is that, at the stage where the band is the circumcircle of the packing of six circles, the configuration is not unique. If one of the circles at the boundary is fixed, then the other four can move around the central one.

3.2. $n = 4$

Let us start with the densest finite packing (Fig. 3(a)). If we want to introduce pressure in this configuration, we find that the system does not take pressure but avoids it by increasing its area A with keeping the length of the perimeter unchanged. The rhombus formed by the four circles continuously changes its

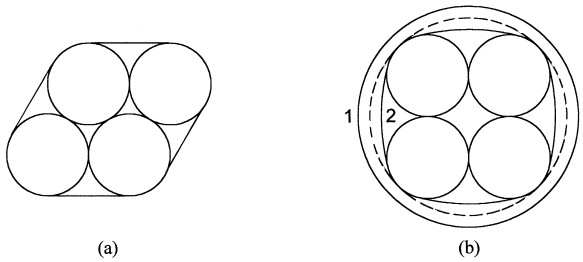

Fig. 3. Packing of four equal circles: (a) with convex hull of minimum perimeter and minimum area and (b) under internal pressure.

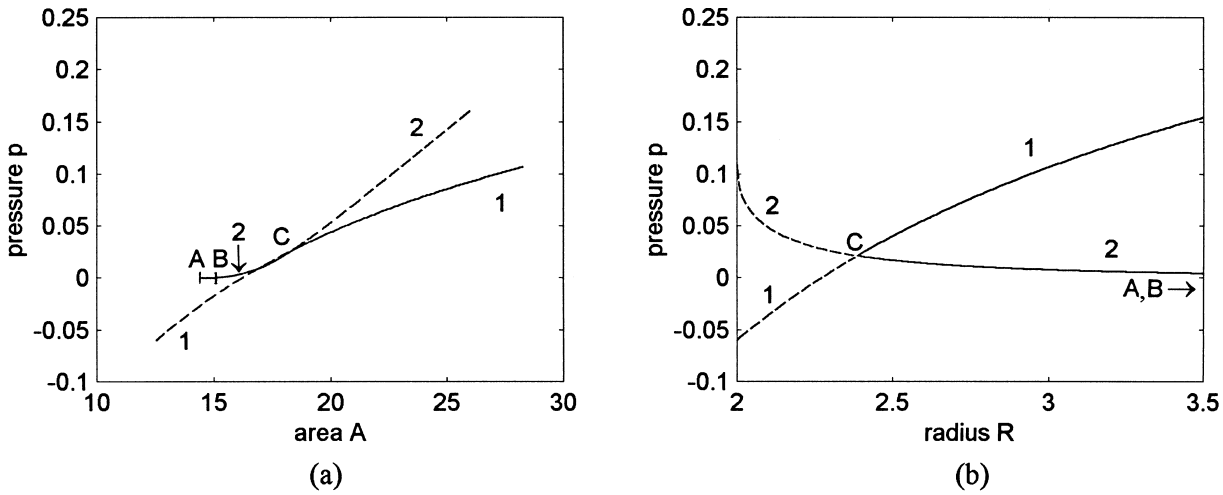

Fig. 4. $n = 4$: equilibrium paths – change of shape of the elastic band under internal pressure. Variation of (a) area with pressure and (b) radius with pressure. The invalid segments of the paths are indicated with dashed lines.

shape to a square, and area A changes according to Eq. (10). The horizontal plateau of curve 2 between points A and B in Fig. 4(a) shows this change. Using Eqs. (6), (7) and (9), in the square form, we can increase pressure p while radius R of the band decreases and area A enclosed by the band increases (curves 2 in Figs. 3(b), 4(a) and (b)). This process is kept going until the band takes the shape of the circumcircle of the packing of the four circles (dashed circle in Fig. 3(b), point C in Figs. 4(a) and (b)), which is just the mathematical packing model of the pattern for four carpels. From now on, a further increase in pressure p results in a circular shape of the band with an increasing radius R (curves 1 in Figs. 3(b), 4(a) and (b)), and the four circles will rattle in the large circle. By decreasing the pressure, we move along the same continuous lines of Figs. 4(a) and (b) as before, but now in the reverse direction. Similar properties characterize the configurations for $n = 5$ and 8.

3.3. $n = 9$

Under no pressure, with an increasing area A, the configuration changes from a hexagonal form (Fig. 5(a)) to a heptagonal form (Fig. 5(b)). This transition is shown by the horizontal plateau of curve 1 between points A and B in Figs. 7(a) and 8. We can increase pressure p while radius R decreases and area A increases

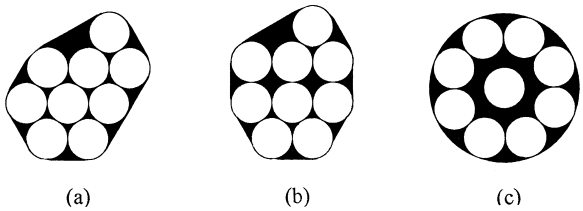

Fig. 5. $n = 9$: equilibrium configurations – explanation of (a)–(c) in text.

(curve 1 in Figs. 7(a), (b), and 8). During this process, the circle arrangement in Fig. 5(b) remains constant, but the band changes its profile. As a consequence of decreasing R, the magnitude of forces $F_i (i = 1, 2, 4, 5, 7, 8, 9)$ in Fig. 6 is changing. The direction of forces F_1 and F_2 is also changing but, because of local symmetry, the direction of the rest of the forces remains unchanged. Change in forces F_i leads to change of forces in members of the truss. With an increase in pressure p, the magnitude of compressive forces in bars between joints 3 and 4, 5 and 6, 6 and 7 gradually decrease. This happens until $p = 0.00134538$, for which the forces in the above-mentioned bars vanish. This state occurs at point C of curve 1 in Figs. 7(a), (b) and 8. Any further increase in pressure p would cause tension in those bars; however, this cannot occur because of the unilateral constraints (only compressive forces can arise in members of the truss). Therefore, for higher pressure, the system with the arrangement of circles in Fig. 5(b) cannot be in equilibrium. And indeed, at this particular pressure, that we can call the *critical pressure*, the configuration loses its stability and catastrophically changes its shape from a heptagonal to an octagonal arrangement (jumps from point C to point D in Fig. 7(a)). To help better understanding, in Fig. 8, we show a schematic enlargement of that part of Fig. 7(a), and in Table 1 we give the characteristic numerical data. This is a limit point (''snap through'') type loss of stability (Thompson and Hunt, 1973) that reminds us to the ''sausage catastrophe'' in packing theory (Wills, 1998).

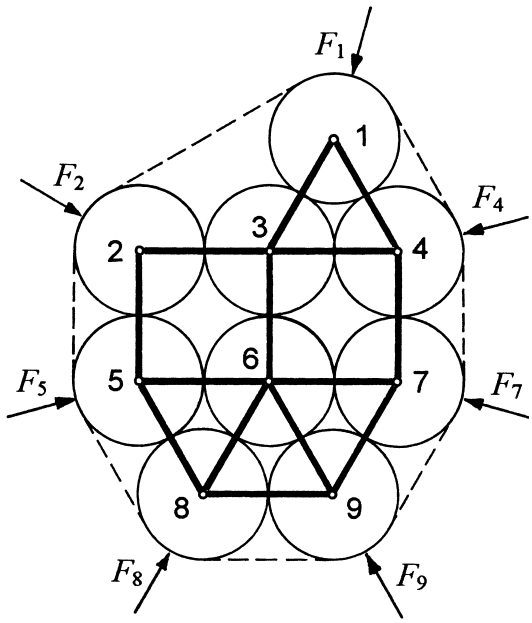

Fig. 6. Graph of circle packing considered as a truss loaded by forces at the boundary.

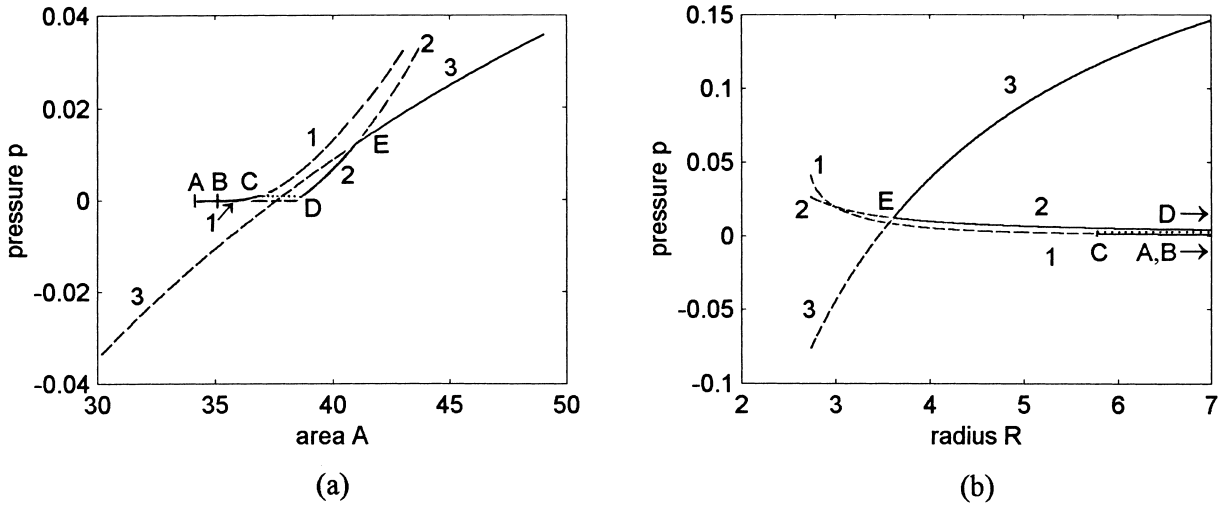

Fig. 7. $n = 9$: equilibrium paths – change of shape of the elastic band under internal pressure. Variation of (a) area with pressure and (b) radius with pressure. The invalid segments of the paths are indicated with dashed lines.

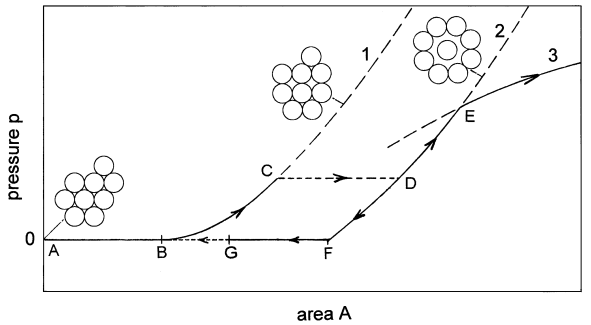

Fig. 8. Variation of area with pressure for nine circles (the invalid segments of the curves are shown with dashed lines). Related data are in Table 1.

Table 1
State characteristics of the assembly of nine circles at characteristic points of the equilibrium path

Point	Pressure p	Area A	Radius R	Length L	Force S
A	0	34.19515	∞	21.74729	0
B	0	35.26595	∞	21.74729	0
C	0.00134538	37.03588	5.788340	21.91664	0.0077875
D	0.00134538	38.76706	18.610382	22.29180	0.0250380
E	0.01214946	41.01248	3.613126	22.70194	0.2758164
F	0	38.45530	∞	22.28318	0.0246421
G	0	a	∞	22.28318	0.0246421

a: $34.58257 \leqslant A \leqslant 37.59337$.

In the new configuration, eight circles are sitting at the vertices of a regular octagon, while the ninth circle is rattling inside the octagon. In the octagon form, we can increase pressure p further while radius R decreases and area A increases (curves 2 in Figs. 7(a), (b) and 8). This process is kept going until the band

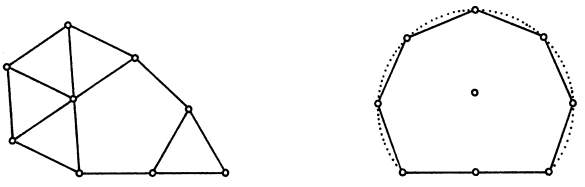

Fig. 9. Graph of packing of nine circles forming a convex polygon with three consecutive vertices lying on a straight line. The polygon with (a) minimum and (b) maximum areas.

takes the shape of the circumcircle of the packing of the nine circles (Fig. 5(c), point E in Figs. 7(a), (b) and 8), which is just the mathematical packing model of the pattern for nine carpels. From now on, a further increase in pressure p results in a circular shape of the band with increasing radius R (curves 3 in Figs. 7(a), (b) and 8), and the nine circles will rattle in the large circle. By decreasing the pressure, below point E, a hysteresis loop is obtained. First, we move along curve 2 until we reach point F (Fig. 8), where there is no internal pressure and the circle arrangement can be in equilibrium in any convex octagonal form. The configuration is in a state of self-stress, because the length of the boundary of the convex hull, which is now L, is greater than the unstrained length L_0 of the elastic band. If we deform a regular octagon, then its area decreases and so does area A of the convex hull of the related circle packing. This means that we move along the horizontal plateau, from point F towards point A. If three consecutive vertices of the octagon are colinear, then the assembly of the circles is in a critical state. The middle one of the three vertices is able to snap inwards the octagon, and the circles return to their initial configuration, marked with point A in Fig. 8. Loss of stability can occur at any point G in the interval $34.58257 \leqslant A \leqslant 37.59337$. The lower bound of this interval refers to the graph of nine circles with three colinear consecutive vertices and with minimum area (Fig. 9(a)), and the upper bound to that with maximum area (Fig. 9(b)). In the latter, the vertices are lying on a circle, representing the solution to the well-known "Dido–Steiner problem" (Pólya, 1968).

4. Conclusions

In the light of the above investigation, it seems that the mathematical packing model of pattern formation of lotus receptacles is rather rigid. It is able to describe only particular configurations as densest packings of equal circles in a circle. The mechanical packing model is much more flexible. It is able to describe more configurations, and there are regions where a continuous change in shape is possible. The greater variety of shapes is in closer agreement with observations in nature.

In the mechanical model, at the internal pressure for which the contact forces between circles vanish, the circles form a locally densest packing in a circle. For $n < 10$, it was found that the local optimum obtained in this way is at the same time a global optimum. So, the configuration obtained is the same as that resulting from the mathematical packing model. Therefore, configurations obtained from the mathematical model are incorporated in the configurations obtained from the mechanical model.

The main feature of the behaviour of nine circles is that, at the critical pressure, the configuration loses its stability and the system undergoes a "snap-through" buckling. This fact is closely related to Green et al. (1996), whose pattern formation theory is based on buckling of tissues.

In most cases, a receptacle with six carpels has a five-fold rotational symmetry and a plane of symmetry. Although both the mathematical model and the mechanical model contain this possibility, neither of them

provides it as a definite, rigid configuration. Improvement of the mechanical model by the introduction of repulsion between circles could overcome this problem.

Acknowledgements

The research reported here has been partially supported by the Hungarian Scientific Research Foundation OTKA Grant No. T024037 and by the Ministry of Education of Hungary FKFP Grant No. 0391/1997. I am grateful to Professor C.R. Calladine for advice and helpful comments.

References

Croft, H.T., Falconer, K.J., Guy, R.K., 1991. Unsolved Problems in Geometry. Springer, New York.

Graham, R.L., Lubachevsky, B.D., Nurmela, K.J., Östergard, P.R.J., 1998. Dense packings of congruent circles in a circle. Discrete Mathematics 181, 139–154.

Green, P.B., 1996. Expression of form and pattern in plants – a role for biophysical fields. Cell and Developmental Biology 7, 903–911.

Green, P.B., Steele, C.S., Rennich, S.C., 1996. Phyllotactic patterns: a biophysical mechanism for their origin. Annals of Botany 77, 515–527.

Hooke, R., 1665. Micrographia: or some physiological descriptions of minute bodies made by magnifying glasses with observations and inquiries thereupon. Jo. Martyn and Ja. Allestry, Printers to the Royal Society, London.

Irvine, H.M., 1981. Cable Structures. The MIT Press, Cambridge, MA.

Jean, R.V., 1994. Phyllotaxis: A Systematic Study in Plant Morphogenesis. Cambridge University Press, Cambridge.

Lian, Z.G., 1987. The Lotus of China. Wuhan Institute of Botany, Chinese Academy of Sciences, Science Press, Beijing (in Chinese).

Pólya, G., 1968. Mathematics and Plausible Reasoning. vol. I. Induction and Analogy in Mathematics. second edn. Princeton University Press, NJ.

Prusinkiewicz, P., Lindenmayer, A., 1990. The Algorithmic Beauty of Plants. Springer, New York.

Tarnai, T., 1997. Packing of equal circles in a circle. In: Chilton, J.C., Choo, B.S., Lewis, W.J., Popovic, O. (Eds.), Structural Morphology – Towards the New Millennium, Proceedings of the IASS International Colloquium, Nottingham.

Tarnai, T., Gáspár, Zs., 1995–1996. Packing of equal circles in a square. Acta Technica Academiae Scientiarum Hungaricae 107 (1–2), 123–135.

Thompson, J.M.T., Hunt, G.W., 1973. A General Theory of Elastic Stability. Wiley, London.

Thornley, J.H.M., 1975. Phyllotaxis. I. A mechanistic model. Annals of Botany 39, 491–507.

Turing, A.M., 1952. The chemical basis of morphogenesis. Philosophical Transactions of the Royal Society of London, Series B 237, 37–72.

Watanabe, S., 1990. The Fascinating World of Lotus. Parks and Open Space Association of Japan, Tokyo, p. 127.

Wills, J.M., 1998. Spheres and sausages, crystals and catastrophes – and a joint packing theory. Mathematical Intelligencer 20, 16–21.